Journal of $CO_2$ Utilization 22 (2017) 117–123

Contents lists available at ScienceDirect

Journal of $CO_2$ Utilization

journal homepage: www.elsevier.com/locate/jcou

# Efficient production of formic acid by simultaneous photoreduction of bicarbonate and oxidation of glycerol on gold-$TiO_2$ composite under solar light

Hanqing Pan[a], Alexzander Steiniger[b], Michael D. Heagy[a], Sanchari Chowdhury[b,c,*]

[a] Department of Chemistry, New Mexico Institute of Mining and Technology, Socorro, NM 87801, United States
[b] Department of Chemical Engineering, New Mexico Institute of Mining and Technology, Socorro, NM 87801, United States
[c] Material Science and Engineering, New Mexico Institute of Mining and Technology, Socorro, NM 87801, United States

ARTICLE INFO

*Keywords:*
Bicarbonate
Plasmonic
Formate
Solar
Glycerol

ABSTRACT

In this paper, we report the efficient production of formic acid through simultaneous photoreduction of bicarbonate and oxidation of glycerol in the presence of gold-$TiO_2$ composite. Under solar light (solar simulator, AM 1.5 filter) the productivity of formate was 0.9 mmol/g cat-hr using $TiO_2$ alone. The yield of formate was remarkably enhanced (7 mmol/g cat-hr) by combining plasmonic gold nanoparticles with $TiO_2$. It was found that in the photocatalytic reaction, glycerol not only serves as an efficient hole sinks but also the oxidation of glycerol may produce additional formic acid further enhancing the overall productivity. When illuminated with 365 nm photon with energy sufficient to excite valence band to conduction band electronic transitions in the $TiO_2$, the productivity of $TiO_2$ alone dramatically improves in comparison to solar light. However, no effect of gold nanoparticles was observed under 365 nm irradiation. The improvement in product yield under solar light is attributed to the synergistic effect of strong plasmonic properties of gold nanoparticles in the visible wavelength range and superior hole scavenging activities of glycerol from gold-$TiO_2$ composite surface.

## 1. Introduction

Formic acid (HCOOH) has been identified as an ideal hydrogen storage material because of its volumetric hydrogen density of 53 g of $H_2$ per liter [1]. This material has low toxicity and is a high energy density liquid under ambient conditions [2]. Formic acid, apart from being an established hydrogen storage material it is also a valuable chemical commonly used as animal feedstock and in leather & textile, rubber, chemical & pharmaceuticals industries preservative. The high demand of formic acid is evident from its growing market (5% growth from 2014 to 2019) and the increasing price [3]. Additionally, formic acid is an intermediate species for many valuable chemicals including methanol. Development of a catalyst to produce formic acid efficiently can open up a door for further research to develop the catalyst to selectively transform $CO_2$ into other valued added chemicals such as alcohols [4]. There are several examples of production of formic acid by the photoreduction of $CO_2$ reported in literature [5–7]. However, the high reduction potentials required for the reaction requires photocatalytic semiconducting materials with higher bandgap energies; hence these catalytic materials can absorb light only in the UV region leaving most of the solar spectrum unused. Many possible products from $CO_2$ reduction (such as oxalic acid, formic acid, formaldehyde, methanol, carbon monoxide, methane, and also some C2–C4 saturated and unsaturated hydrocarbons) make it challenging to enhance the selectivity and yield of formic acid [8]. Moreover, the limited solubility of $CO_2$ in water (0.033 M at 298 K and 1 atm), coupled with the use of aqueous reactant solvents poses a practical disadvantage [9]. This limitation has been partially eliminated by dissolving $CO_2$ in an aqueous solvent at high pressure. A recent study by Leonard et al. has shown that in the case of reactant solution involving $CO_2$ and bicarbonate, bicarbonate is the predominate species undergoing reduction [10]. This finding is a useful observation since $CO_2$ can be captured efficiently in the form of $NaHCO_3$ using different sorbent materials like sodium metasilicate and encapsulated liquid sorbent [11,12].

$TiO_2$ has been identified as one of the most efficient catalysts for the reduction of $CO_2$ due to its suitable conduction and valence band edge potentials. However, owing to the short wavelength cutoff of $TiO_2$ absorption, only a small fraction of solar photons (~4%) can be utilized to excite this photocatalyst resulting in low photocatalytic yield. In addition, $TiO_2$ can oxidize water to form hydroxyl radicals which can adversely affect the desired product formation by $CO_2$ reduction. The strongly oxidizing hydroxyl radicals may readily react with some

* Corresponding author at: Department of Chemical Engineering, New Mexico Institute of Mining and Technology, Socorro, NM 87801, United States.
*E-mail address:* sanchari.chowdhury@nmt.edu (S. Chowdhury).

http://dx.doi.org/10.1016/j.jcou.2017.09.016
Received 25 June 2017; Received in revised form 13 September 2017; Accepted 21 September 2017
Available online 30 September 2017
2212-9820/ Published by Elsevier Ltd.

intermediates thereby hindering the process before the six- or eight-electron reduction products are obtained [8]. It has been reported that during the photocatalytic reduction of $HCO_3^-$ to formate, the amount of · OH radicals from the photo-oxidation of water shows a linear dependence on the concentration of bicarbonate. Strongly oxidizing hydroxyl radicals can oxidize bicarbonate to carbonate, an undesired side reaction which can compete with the reduction path to form formate. This can reduce the overall yield of formate production [13]. This highlights the importance of a sacrificial hole-scavenger in any $TiO_2$-mediated photochemical reduction.

The photocatalytic reduction of high-pressure $CO_2$ to produce methane and formic acid using $TiO_2$ powders with 2-propanol as a positive hole scavenger has been previously reported [7]. Under their optimum experimental conditions, the production rate of formic acid was a mere 0.46 μmol · $(g\text{-}Ti)^{-1}$ $h^{-1}$. Recently, zinc sulfide was proven to be a promising catalyst for the photoreduction of bicarbonate to formic acid in the presence of positive hole scavengers like 2-propanol, ethylene glycol, and glycerol. While the redox potentials of these solvents are similar (ethylene glycol 0.76 V, 2-propanol 0.80 V and glycerol 0.79 V)., glycerol was shown to be most efficient hole scavenger for the reaction [10]. It was found that under air mass coefficient zero (AM 0) solar spectrum conditions, applying wurtzite ZnS nanoparticles as a photocatalyst in conjunction with glycerol as hole-scavenger, the productivity of formic acid can be obtained as high as 3.5 mmol/g cat-hr. It was suggested that glycerol contains one secondary and two primary alcohol groups; all of which are potential sites for oxidation that could enhance the hole scavenging activity. Density-functional based theoretical work by Fittipaldi et al. also established glycerol as a most efficient hole scavenger for $TiO_2$ when compared to other organic solvents like that-butanol, 2-propanol methanol, and formic acid [14]. In contrast to petroleum derived isopropanol, glycerol is a green solvent which is low cost, environmentally benign, relatively abundant, and a plant-derived solvent [15,16].

Designing photocatalysts with plasmonic nanostructures is an attractive approach to design visible-light-responsive photocatalysts [17]. Plasmonic nanoparticles such as gold and silver have been widely used for improving the photocatalytic efficiency of $TiO_2$ due to their visible light absorption and intense plasmonic properties. Gold nanostructures can strongly interact with visible light at resonant frequencies resulting in excited plasmons, which can dephase following different pathways. The plasmons can decay radiatively reemitting photons and concentrate electromagnetic field at the molecular scale. Surface plasmons at the metal can also relax non-radiatively creating a transient population of non-equilibrium (hot) charge-carriers or by releasing thermal energy [18]. The hot electrons can be transferred to the conduction band of $TiO_2$. The localization of electromagnetic fields close to the Au/$TiO_2$ interface and the enhanced supply of electrons to $TiO_2$ conduction band can improve the overall photocatalytic efficiency of the system [17]. Applications of metallic nanoparticles have been explored previously to improve $CO_2$ reduction. For example, the enhanced photocatalytic reduction of $CO_2$ to methanol was demonstrated on the surface of Cu-modified $TiO_2$ nano-flower films under UV light [19]. and Ag/$TiO_2$ nanowire film under visible light [20]. Similarly, the Au/$TiO_2$ composite [21] and Au–Cu alloy nanoparticles/$TiO_2$ composite [22] are demonstrated to increase the photoreduction of $CO_2$ with $H_2O$ to produce $CH_4$ under visible-light irradiation. Photoconversion of $CO_2$ to CO was effectively achieved by hydrous hydrazine on $SrTiO_3$/$TiO_2$ coaxial nanotube arrays loaded with Au-Cu alloy nanoparticles [23]. Recently, Lim et al. reported enhanced photoconversion of $CO_2$ into formic acid under visible light using reduced graphene-coated gold nanoparticles, which is attributed to the hot electron transfer from plasmonic gold nanoparticles to graphene [24].

In this paper, we report the first demonstration of coupling plasmon enhanced photoreduction of bicarbonate with oxidation of glycerol to realize the highly efficient one-pot production of formic acid using gold-$TiO_2$ as a photocatalyst. Our study compares the efficiency of 2-propanol and glycerol as the hole-scavenging agent for the above reaction system. We discover a notable increase in the formate production under the solar light when gold/$TiO_2$ composite is applied in conjunction with glycerol. This work demonstrates the highest reported productivity to date at 7 mmol/g cat-hr under solar light. We compare the effect of gold nanoparticles on the photoreactivity of $TiO_2$ under solar, visible (> 400 nm), and UV (365 nm) ilumination. This study indicates that the improvement of photocatalytic effect in the solar light is caused by the plasmonic effect of gold nanoparticles in the visible wavelength range. To gain a better insight into the role of gold to influence the photocatalytic effect of $TiO_2$, we also assess the hydroxyl radical production and photo-reduction of resazurin.

## 2. Experimental procedures

### 2.1. Materials

Titanium dioxide ($TiO_2$) nanopowder (Aeroxide® P25) was purchased from Sigma-Aldrich. According to the manufacturer's data, $TiO_2$ has a specific surface area of 35–65 $m^2/g$ (BET) and a mean diameter of 21 nm. The sizes of $TiO_2$ nanoparticles were later confirmed by our TEM data. Gold nanoparticles were synthesized by well-established methods in which the gold salt precursor hydrogen tetrachloroaurate trihydrate, ($HAuCl_4$ •$3H_2O$) is reduced by trisodium citrate dihydrate, $Na_3C_6H_5O_7$•$2H_2O$ [25]. The nanoparticles were characterized by TEM and Thermo Scientific Evolution™ 300 UV–vis Spectrophotometer equipped with the integrated sphere.

### 2.2. Photocatalytic reactions

For bicarbonate to formate reaction, a buffer made of 0.3 M $NaHCO_3$, 2 M hole scavenger (2-propanol or glycerol), and Milli-Q water was used as the starting reactant solution. The loading of $TiO_2$ nanocatalyst was first varied from 0.01 mg/mL to 1 mg/ mL, to find the optimum value. We found that increasing the loading of $TiO_2$ beyond 0.1 mg/mL does not improve the action rate and at 1 mg/mL, the productivity decreases due to the aggregation of $TiO_2$. Finally, for all our photocatalytic experiments the loading of $TiO_2$ was maintained at 0.1 mg/mL (approximately $5 \times 10^{12}$ particles/mL). Au nanoparticles were added to $TiO_2$ at a loading of 4 wt percent. Photocatalysts were added to the reactant solution and were stirred in the dark for overnight to reach adsorption equilibrium. The photocatalytic reaction occurred in a quartz tube, sealed, and placed under a light source for 8 h. Aliquots were collected at two-hour increments, and formate concentration was quantified by ion chromatography. Ion chromatography was performed on a Dionex AS50 IC with a Dionex IonPac ICE-AS6 ion exclusion column and a Thermo Scientific Dionex AMMS-ICE 300 suppressor. The IC instrument is equipped with a Dionex CD25 conductivity detector. Reagents used were 0.4 mM heptafluorobutyric acid as the eluent at a flow rate of 1.2 mL/min and 5 mM tetrabutylammonium hydroxide as the regenerate. A control experiment was performed with only glycerol and photocatalyst (Au, $TiO_2$, and Au/$TiO_2$). A 2 M solution of glycerol was made with Milli-Q water, and the pH was adjusted to 9 with 6 M NaOH. This was done under solar illumination and 365 nm irradiation.

We investigated the ability of the $TiO_2$-Au composite in catalyzing the reduction of resazurin (VWR Scientific) to resorufin in water at room temperature under visible and 365 nm photon sources. 2 mL of resazurin (8 micromolar) is mixed with 10 microliters of glycerol. The reaction is initiated by adding $TiO_2$ or gold-$TiO_2$ to the solution and by illuminating with light. The progression of reaction is studied by monitoring the UV–vis absorption peak. Upon reaction, the solution color turns from blue (resazurin) to pink (resorufin) gradually.

All the photocatalytic reactions were conducted under three different light inputs, solar light, visible light and 365 nm photons. For solar light, an ABET Technologies SunLite™ solar simulator with AM 1.5

filter and a 1000 W xenon arc lamp were used. A 365 nm uniform light source was custom-built using Mouser Electronics LED with FWHM of 15 nm. The visible light source was accomplished by implementing a 400 nm long pass filter with a halogen lamp. For all the light sources, the similar power output of 100 mW/cm$^2$ power output the equivalent of one sun was used. The quartz tube reactor can transmit 90% of the solar light incident on its outer wall. Considering that, we can approximate the light intensity at the inner wall of the quartz tube or at the glass liquid interface to be 90 mW/cm$^2$. All the reactions were carried out at controlled room temperature to exclude thermal effects on the reaction rate.

### 2.3. Hydroxyl radical monitoring reaction

Terephthalic acid (TA) was used to monitor the hydroxyl radical generation in different reaction conditions. The hydroxyl radical can convert terephthalic acid to fluorescent 2-hydroxy terephthalic acid (HTA) [26]. These molecules are fully compatible with nanoparticles as it does not induce any aggregation. It is a very sensitive technique allowing the detection limit of 30 nM of hydroxyl radicals.

### 2.4. Apparent quantum efficiency (AQE)

Using an Ophir Photonics Nova II laser energy meter, the energy output of the solar simulator was measured. This power measurement was converted to moles of photons per second. This photon flux was then used to calculate the apparent quantum efficiency (AQE) of the catalyst using Eqs. (1) and (2). The detailed calculation procedure is mentioned in the Supplementary information.

$$theoreticalmol\ \ formate = nmol\ \ protons \cdot \frac{1\ \ mole^-}{mol\ \ photons} \cdot \frac{mol\ \ formate}{2\ \ mole^-} \quad (1)$$

$$AQE = \frac{actual\ \ mol\ \ formate}{theoretical\ \ mol\ \ formate} \cdot 100 \quad (2)$$

## 3. Results and discussion

### 3.1. Gold/$TiO_2$ characterization

In this study, Degussa P25 $TiO_2$ nanocatalyst was chosen, which is widely used photocatalyst due to their high catalytic efficiency. P25 usually contains more than 70% anatase with a minor amount of rutile and a small amount of amorphous phase. The average size of $TiO_2$ nanoparticles provided by the supplier is 21 nm, however, in our reaction solution, $TiO_2$ is mostly present as aggregate (Fig. 1b) due to its poor solubility in aqueous solution. The average size of gold nanoparticles was 13 nm, and in aqueous solution, they showed a plasmonic peak at 523 nm (Fig. 1(a) and (c)). $TiO_2$ nanoparticles have absorbance peak around 350 nm (Fig. 1c), and diffusion reflectance data confirm bandgap of 3.2 eV (Fig. S3, Supplementary). Gold nanoparticles/$TiO_2$ composites are prepared by simply mixing and then placing in a sonicator for 30 min. The TEM image reveals that gold nanoparticles get attached to $TiO_2$ nanoparticles (Fig. 1(b). However, part of the gold nanoparticles aggregates in bicarbonate buffer solution as can be seen by both TEM image and absorbance spectra (Fig. 1). As shown in Fig. 1c, upon aggregation, the absorption intensity of gold exhibited a decrease at 527 nm and an increase at a higher wavelength (around 750 nm). Upon attachment to gold nanoparticles, a slight change in the absorbance of $TiO_2$ was observed. This result confirms that the addition of Au is unlikely to cause any significant screening effect.

### 3.2. Photocatalytic activity

#### 3.2.1. Formate production

Relevant reactions involved for formate at the $TiO_2$ surface in the presence of glycerol can be expressed as follows [13]:

$$TiO_2 + h\nu(UV) \rightarrow TiO_2(e^-_{cb} + h^+_{vb}) \quad (1)$$

$$TiO_2(h^+_{vb}) + H_2O \rightarrow TiO_2 + H^+ + {}^\circ OH \quad (2)$$

$$TiO_2(e^-_{cb}) + O_2 \rightarrow TiO_2 + O_2^- \quad (3)$$

$$HCO_3^- + 2e^-_{cb} + 2H^+ \rightarrow HCO_2^- + H_2O \quad (4)$$

$$HCO_3^- + {}^\circ OH \rightarrow {}^\circ CO_3^- + H_2O \quad (5)$$

As shown above in reaction 2, the $HCO_3^-$ ion is reduced to formate by photogenerated electrons at the conduction band of $TiO_2$. EPR spin trapping experiments conducted by Amadelli et al. suggested that the amount of · OH radicals from the photo-oxidation of water is directly proportional to the concentration of bicarbonate in solution [13]. The electron scavenging by $HCO_3^-$ increases the lifetime of holes on the $TiO_2$ surface. However, photo-oxidation of bicarbonate to carbonate (reaction 5) can compete with its reduction to form formate (reaction 4). It is evident that along with an enhanced supply of electrons, elimination of holes and hydroxyl radicals is important to improve the yield of formate. Under solar simulator $TiO_2$ alone has the productivity of 0.9 mmol formate/g cat-hr in the presence of glycerol as a hole scavenger, but productivity is negligible when 2-propanol is used (Fig. 2(a)). The superiority of glycerol as a hole scavenger can be explained by the fact that glycerol possesses more primary OH groups, which leads to the improved C—H hole scavenging reactivity. Glycerol has three hydroxyl groups and can be adsorbed more strongly on $TiO_2$ in comparison to 2-propanol. Additionally, polyhydroxy structures favored efficient transferring of photo-generated holes in $TiO_2$ to the adsorbed glycerol, which could suppress the charge carrier recombination and promote the photoreduction [27]. To confirm the effect of glycerol we performed experiments with three different concentration of glycerol (2 M, 0.03 M and 0.003 M) and with the same amount of the $TiO_2$ and the bicarbonate in the reactant solution under solar light. The formate production was 0.9, 0.7 and 0.4 mmol formate/g cat-hr, respectively. As evident, the formate production rate decreases with the decrease in the concentration of glycerol in the reactant solution. This confirms that the photoreduction efficiency of $TiO_2$ is

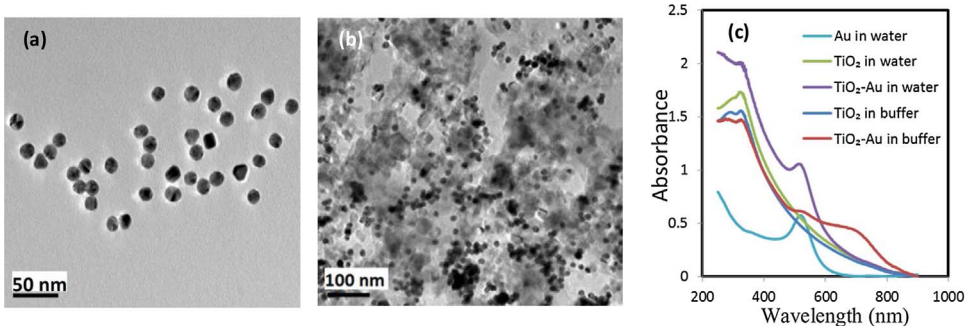


**Fig. 1.** (a) TEM image of gold nanoparticles (b) TEM image of gold nanoparticles/$TiO_2$ nanocatalyst in glycerol-bicarbonate buffer solution (c) UV–vis absorbance of gold nanoparticles and $TiO_2$ in water and buffer solution (color required).

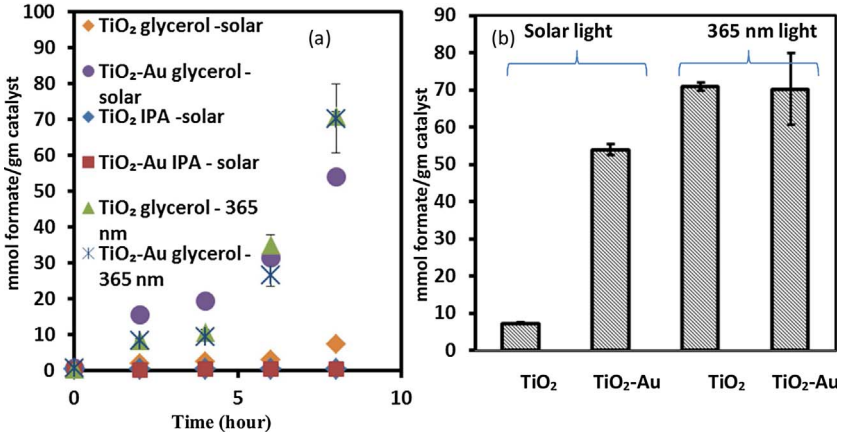


**Fig. 2.** (a) Time course of formate production using the hole scavenger isopropyl alcohol and glycerol under solar light and 365 nm light. (color required) (b) Photocatalytic product yields (after 8 h of irradiation) on $TiO_2$ and $TiO_2$-gold in the presence of glycerol.

strongly dependent on the concentration of glycerol, hence the number of OH groups.

Under 365 nm light the production yield of formate in the presence of $TiO_2$ and glycerol is significantly higher (Fig. 2) than the productivity under solar simulator. This can be understood from the fact that only 4% of the solar spectrum has energy high enough to induce electron-hole pair excitations in $TiO_2$. In contrast, the photon energy at 365 nm wavelength is higher than the bandgap energy of $TiO_2$. As a result, all the photon energy from UV light can be utilized to excite the electrons from valence band to conduction band in $TiO_2$. The photogenerated electrons at the conduction band of $TiO_2$ reduce bicarbonate to formate where glycerol efficiently scavenges the holes.

### 3.2.2. *Application of gold nanoparticles*

In addition to the isolated gold nanoparticle plasmon resonance at 500 nm, partially aggregated nanoparticle showed an extended plasmon broadband absorption in the 550–800 nm region (Fig. 1c). The electromagnetic field can be localized in subwavelength regions within nanoparticle aggregates creating plasmonic hotspots [28]. Under solar irradiation, gold nanoparticles enhance the production yield of formate eight-fold (Fig. 2(a), Table 1). Since the spectral overlap is minimum between $TiO_2$ and gold, observed improvement cannot be solely explained by increased light absorption on $TiO_2$ due to plasmon-induced resonance energy transfer from gold to $TiO_2$ [29]. Plasmonic heating cannot be the main reason for observed enhancement effect either since $CO_2$ to formate requires the energy of 0.61 V, which is higher than the thermal energy generated by plasmonic heating under solar light [8,29]. While the other effects, cannot be completely excluded, the plasmon induced hot electron transfer from gold nanoparticles to $TiO_2$ seems to play a most important role here. (Fig. 3).

The enhanced productivity of formate and the improved quantum efficienmcy values in the presence of $TiO_2$/Au gold nanocomposite can be attributed to the synergistic effect of strong plasmonic properties of gold nanoparticles in the visible wavelength range and superior hole scavenging activities of glycerol from both gold and $TiO_2$ surfaces. These photoexcited plasmons in gold nanoparticles can decay non-radiatively, creating a transient population of non-equilibrium (hot) charge carriers which can be eventually transferred to the conduction band of $TiO_2$ to enhance the photochemical reactions on its surface. However this hot electron transfer process is often inefficient as the photo excited electrons in metal can quickly recombine with the holes

**Table 1**
Apparent quantum efficiency of formate production in glycerol.

| | Solar light | 365 nm |
|---|---|---|
| $TiO_2$ | 0.3% | 9.2% |
| $TiO_2$/Au NPs | 2.4% | 9.4% |

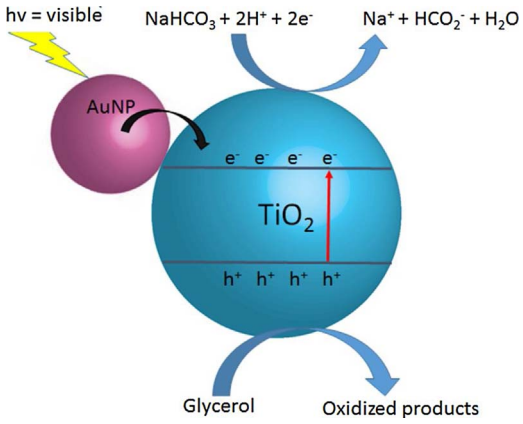


**Fig. 3.** Schematic representation of formate production on gold-TiO2 composite under solar light.

due to the absence of bandgap. Application of suitable hole scavenger like glycerol can scavenge the holes from both $TiO_2$ and gold nanoparticles by an oxidation process resulting in enhancement in overall supplies of electrons hence can significantly increase the efficiency of the photoreduction process [29,30].

To confirm the plasmonic effect of gold nanoparticles to be essential for enhanced productivity of formate, we performed the experiment with gold/$TiO_2$ under 365 nm irradiation at which the plasmonic effect of gold nanoparticles is absent (Fig. 2). As expected, under UV light no effect of gold nanoparticles on the productivity of $TiO_2$ was observed. When gold is illuminated with 365 nm UV light, the enhancement efficiency is negligible due to two main reasons. First, the photon absorbance of gold nanoparticles is low at that wavelength (Fig. 2). Second, most of the photons absorbed at that wavelength are wasted in interband transition (interband energy ~2.3ev), resulting in the generation of hot electrons with low energy. The light absorbed above ~539 nm will be mostly utilized to generate highly energetic hot electrons which can be transferred to $TiO_2$ to enhance the photoreduction process. Due to that obvious reason gold nanoparticles greatly enhanced formate production under solar irradiation (in the visible wavelength range) but not at 365 nm wavelength [31].

Interestingly, we found that gold nanoparticles in buffer solution remain stable during reaction time under solar light but degrade significantly under 365 nm irradiation (Fig. 4). It should also be noted that gold nanoparticles remain stable in water $TiO_2$ solution under both light conditions (Fig. 4a). At 365 nm irradiation, all the electrons available for the reduction reaction are excited from the valence band of $TiO_2$, leaving an equal number of holes behind. In this case, the amount of · OH radicals from the photo-oxidation of water is expected to be directly proportional to the concentration of bicarbonate in

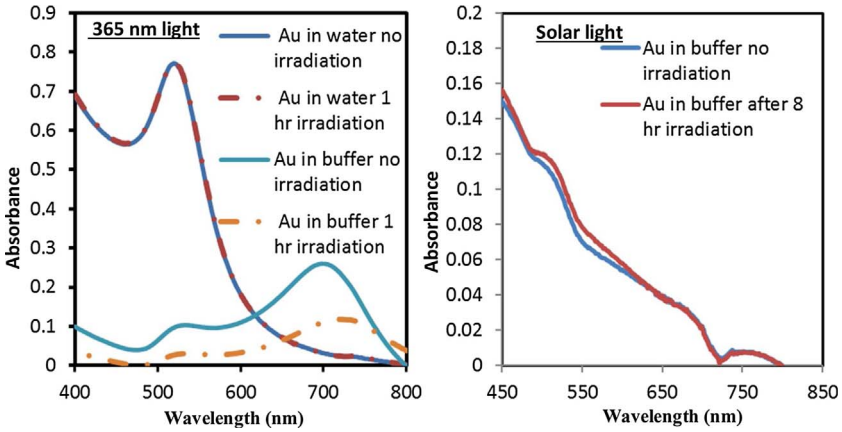


**Fig. 4.** UV–vis absorbance of gold nanoparticles in $TiO_2$ aqueous solution and $TiO_2$ glycerol bicarbonate buffer solution under (a) 365 nm light (b) solar light (color required for both a and b).

solution [13]. Glycerol can scavenge most holes formed on $TiO_2$. However, around 10% of holes remain un-scavenged even at high concentration of the hole scavenger (> 10 vol.%) as noted by Shkrob et al. [32]. The unscavenged holes can react with the gold nanoparticles and can oxidize those gold nanoparticles [33,34]. This agrees with the observation of Kamat et al. [33]. They reported that continuous irradiation of the $TiO_2$- gold composite films with UV light over a long period causes photocurrent to decrease due to photoinduced chemical changes occurring at the gold/$TiO_2$ interface. The degradation of the gold $TiO_2$ composite was attributed to the hole and/or · OH, radical mediated oxidation of gold nanoparticles at the $TiO_2$ interface to produce Au+ ions. The redox potentials of holes (+2.5 V vs. NHE) and hydroxyl radicals (+1.9 V vs. NHE) thermodynamically favor oxidation of gold ((Au0/Au+), 1.68 V vs. NHE). $Au^+$ ions can be reduced to Au by photogenerated electrons on the $TiO_2$ surface. Hence gold nanoparticles can serve as recombination centers resulting in the net loss of electrons during long-term irradiation experiments.

We also examined the possibility of formic acid formation due to the oxidation of glycerol alone. A control experiment was performed with only glycerol on $TiO_2$ or Au/$TiO_2$ samples. Our results indicated that glycerol could be converted into formate simultaneously when bicarbonate was transformed into formate (Fig. 5). It should be noted that the formate produced in the presence of glycerol alone is significantly lower than formate produced in the presence of both bicarbonate and glycerol together. We realized there might be other value added chemicals produced by glycerol oxidation. However, in this work, we only kept track of formic acid formation as that was our product of interest.

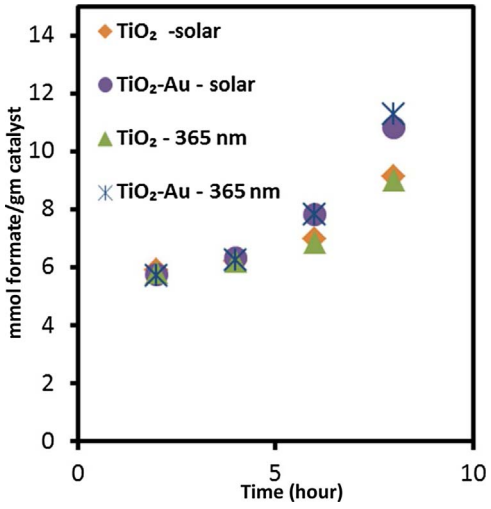


**Fig. 5.** Formate production from glycerol alone using $TiO_2$ or $TiO_2$-gold composite (color required).

Under photoirradiation, glycerol was likely first dehydrogenated to glyceraldehyde and 1,3-dihydroxyacetone. In sequence, glyceraldehyde and 1,3-dihydroxyacetone can be further oxidized by photoexcited holes with water to hydroacetic acid and formic acid through C − C bond cleavage [27,35]. Interestingly we did not see any effect of wavelength dependence on the formate production from $TiO_2$ or $TiO_2$/gold. It is also plausible that the glycerol oxidation to formic acid occurred catalytically on $TiO_2$ and gold/$TiO_2$ because of gold–$TiO_2$ is a typical thermal catalyst for glycerol oxidation [29,36]. The detailed investigation of the glycerol oxidation remains out of the scope of this work.

### 3.2.3. *Resazurin reduction*

To confirm the enhancement effect of gold on photoreduction efficiency of $TiO_2$ under visible light, we studied another reaction. Redox blue dye resazurin is readily and irreversibly reduced by the photogenerated electrons on the $TiO_2$ to pink resorufin. Photogenerated holes on $TiO_2$ can be consumed by a sacrificial electron donor glycerol [37]. The photocatalytic reaction can be presented as follows:

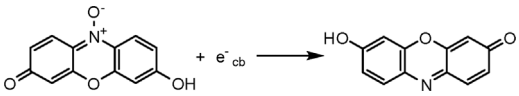


(6)

Resazurin reduction is an established model reaction used to understand photocatalytic reduction efficiency of $TiO_2$ [37]. This reaction can be visually monitored by color change or spectrophotometrically by looking at absorbance peak change. The UV–vis peak of the reaction solution shows a decrease of the resazurin absorption at 600 nm and an increase of the resorufin absorption at 568 nm over time (Fig. S4). Since the resorufin can further degrade to non-absorbing species, the disappearance of resazurin absorbance peak is monitored for reliable prediction of photoreduction rate [38]. Without $TiO_2$, the absorbance peak of resazurin with glycerol did not change under either 365 nm light or visible light exposure. As expected, the photoreduction of resazurin with $TiO_2$ was higher under 365 nm irradiation than visible light (Fig. 6a) and quickly reaches completion within 2 min of the experiment. Similarly, the addition of the gold nanoparticle with $TiO_2$ significantly improved the photoreduction rate of resazurin under visible light and the reaction rate plateau at the end of the 2 min. (Fig. 6a). This observation is consistent with the enhanced bicarbonate reduction with $TiO_2$-gold composite under visible light.

### 3.2.4. *Probing hydroxyl radicals generation*

To further understand the hole scavenging activity of glycerol and 2-propanol in conjunction with gold/$TiO_2$ nanoparticle, we monitored the hydroxyl radical production using terephthalic acid (TA). TA produces a fluorescent product, 2- hydroxy terephthalic acid (HTA) upon oxidation by hydroxyl radical.

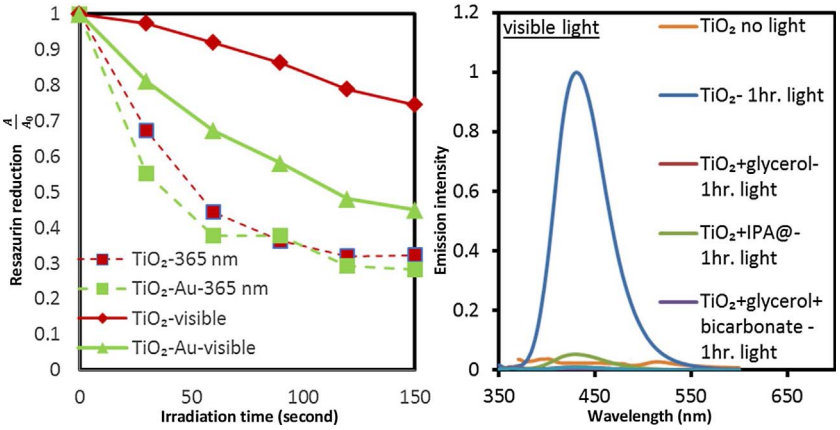


**Fig. 6.** (a) Resazurin reduction with $TiO_2$ and gold nanoparticles observed by observing the change of the absorbance peak of resazurin at 600 nm (b) Hydroxyl radical generation as probed by the emission of HTA when excited with 340 nm light. Emission peak of HTA after 1 h light exposure in TiO2 solution is normalized to one. Other emission spectra are scaled accordingly. (color required).

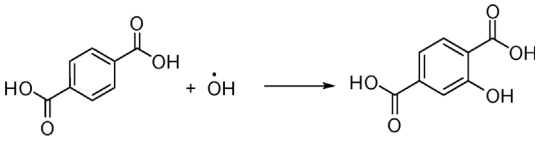

terephthalic acid 2- hydroxy terephthalic acid (10)

When illuminated by either 365 nm wavelength light or visible light, $TiO_2$ alone can produce a significant amount of hydroxyl radicals, as indicated by the fluorescence signal from HTA (Fig. 6(b), Fig. S5). The addition of either glycerol or 2-propanol with $TiO_2$ successfully decreases the production of hydroxyl radicals. These results alone cannot justify significantly higher efficiency of formic acid production in the presence of glycerol in comparison to 2-propanol due to only better hole scavenging effect. This again suggests the possibility of formic acid contribution from glycerol oxidation. It should also be noted that hydroxyl radical probes like terephthalic acid mainly estimates the free · OH radicals in solution. This method may not be reliable to get information about catalyst surface-bound hydroxyl radicals or holes [39]. In the presence of bicarbonate alone or glycerol-bicarbonate combination, the production of hydroxyl radicals by $TiO_2$ in aqueous solution is significantly hindered. Strongly oxidizing hydroxyl radicals may quickly oxidize bicarbonate to produce a carbonate, hence decreasing the yield of hydroxyl radical [13].

## 4. Conclusions

We have studied the photoreactivity of $TiO_2$ nanocatalyst, and gold/$TiO_2$ nanocomposites towards the reduction of $CO_2$ derived bicarbonate to formic acid. Additionally, two different organic positive hole scavengers, petroleum derived 2-propanol, and a promising green solvent glycerol was investigated for their effect on this reaction. Under the solar light, $TiO_2$ alone showed the productivity of formate to be only 0.07 mmol formate/g cat-hr) when using 2-propanol as the hole scavenger. The productivity increased by 15 fold when the glycerol is used as hole scavenger, which established glycerol as a preferable positive hole scavenger. When irradiated with 365 nm UV photons with energy high enough to excite the electrons in $TiO_2$, application of glycerol can increase the productivity of formate to an impressive 9 mmol formate/g cat-hr.

Au nanoparticles loaded $TiO_2$ photocatalyst in the presence glycerol is an efficient material for the solar-light reduction of bicarbonate to formic acid, exhibiting a production rate of 7 mmol formate/g cat-hr. In contrast, the addition of gold nanoparticles with $TiO_2$ nanostructures did not improve the photoreduction of bicarbonate under UV light. The enhanced efficiency of $TiO_2$-gold composite on photoreduction reaction is confirmed with another reaction, the reduction of resazurin under visible light. This shows that the plasmonic properties of gold nanoparticles play an important role in enhancing the photoreduction reactions on $TiO_2$. Gold nanostructures strongly interact with visible light resulting in enhanced electric fields and generation of energetic charge carriers. These energetic electrons can be transferred to the conduction band of $TiO_2$ improving photocatalytic reduction on gold/$TiO_2$ composite. Gold/$TiO_2$ composite can also catalyze the efficient oxidation of glycerol to produce additional formic acid. Hence glycerol can act as a superior hole scavenger for gold/$TiO_2$ composite catalytic system.

In summary, this study provides an efficient method for high yield photocatalytic formate production using gold-$TiO_2$ composite under solar energy. Also, we developed an understanding of the effect of gold nanoparticles on photoreactivity of $TiO_2$ under the different light condition, and its implication with respect to a reduction and as well as an oxidation reaction. We have successfully demonstrated that combination of a suitable hole scavenger and plasmonic nanoparticles can significantly enhance the efficiency of photocatalyst such as $TiO_2$. The understanding developed from this study can be easily extended to improve many other relevant photocatalytic reactions.

## Acknowledgements

Funding for this project was partially provided by NSF Award IIA-1301346 and NM Space Grant Undergraduate Research Fellowship. Authors will also wish to thank Dustin Baca for IC assistance and Ying-Bing Jiang for TEM assistance.

## References

[1] D. Mellmann, P. Sponholz, H. Junge, M. Beller, Formic acid as a hydrogen storage material – development of homogeneous catalysts for selective hydrogen release, Chem. Soc. Rev. 45 (14) (2016) 3954–3988.
[2] B. Loges, A. Boddien, H. Junge, M. Beller, Controlled generation of hydrogen from formic acid amine adducts at room temperature and application in H2/O2 fuel cells, Angew. Chem. Int. Ed. 47 (21) (2008) 3962–3965.
[3] http://www.marketsandmarkets.com/PressReleases/formic-acid.asp.
[4] A. Álvarez, A. Bansode, A. Urakawa, A.V. Bavykina, T.A. Wezendonk, M. Makkee, J. Gascon, F. Kapteijn, Challenges in the greener production of Formates/Formic acid, methanol, and DME by heterogeneously catalyzed CO2 hydrogenation processes, Chem. Rev. 117 (14) (2017) 9804–9838.
[5] L. Cao, S. Sahu, P. Anilkumar, C.E. Bunker, J. Xu, K.A.S. Fernando, P. Wang, E.A. Guliants, K.N. Tackett, Y.-P. Sun, Carbon nanoparticles as visible-light photocatalysts for efficient CO2 conversion and beyond, J. Am. Chem. Soc. 133 (13) (2011) 4754–4757.
[6] G. Yin, H. Abe, R. Kodiyath, S. Ueda, N. Srinivasan, A. Yamaguchi, M. Miyauchi, Selective electro- or photo-reduction of carbon dioxide to formic acid using a Cu-Zn alloy catalyst, J. Mater. Chem. A 5 (2017) 12113–12119.
[7] S. Kaneco, Y. Shimizu, K. Ohta, T. Mizuno, Photocatalytic reduction of high pressure carbon dioxide using TiO2 powders with a positive hole scavenger, J. Photochem. Photobiol. 115 (3) (1998) 223–226.
[8] S.N. Habisreutinger, L. Schmidt-Mende, J.K. Stolarczyk, Photocatalytic reduction of CO2 on TiO2 and other semiconductors, Angew. Chem. Int. Ed. 52 (29) (2013) 7372–7408.
[9] C. Janáky, D. Hursán, B. Endrődi, W. Chanmanee, D. Roy, D. Liu, N.R. de Tacconi, B.H. Dennis, K. Rajeshwar, Electro- and photoreduction of carbon dioxide: the twain shall meet at copper oxide/copper interfaces, ACS Energy Lett. 1 (2) (2016)

332–338.
[10] D.P. Leonard, H. Pan, M.D. Heagy, Photocatalyzed reduction of bicarbonate to formate: effect of ZnS crystal structure and positive hole scavenger, ACS Appl. Mater. Interfaces 117 (2015) 13452–13461.
[11] R. Rodríguez-Mosqueda, H. Pfeiffer, High CO2 capture in sodium metasilicate (Na2SiO3) at low temperatures (30–60 °C) through the CO2–H2O chemisorption process, J. Phys. Chem. C 117 (26) (2013) 13452–13461.
[12] J.J. Vericella, S.E. Baker, J.K. Stolaroff, E.B. Duoss, J.O. Hardin Iv, J. Lewicki, E. Glogowski, W.C. Floyd, C.A. Valdez, W.L. Smith, J.H. Satcher Jr., W.L. Bourcier, C.M. Spadaccini, J.A. Lewis, R.D. Aines, Encapsulated liquid sorbents for carbon dioxide capture, Nat. Commun. 6 (2015) 6124.
[13] A. Molinari, L. Samiolo, R. Amadelli, EPR spin trapping evidence of radical intermediates in the photo-reduction of bicarbonate/CO2 in TiO2 aqueous suspensions, Photochem. Photobiol. Sci. 14 (5) (2015) 1039–1046.
[14] C. Di Valentin, D. Fittipaldi, Hole scavenging by organic adsorbates on the TiO2 surface: a DFT model study, J. Phys. Chem. Lett. 4 (11) (2013) 1901–1906.
[15] A. Wolfson, C. Dlugy, Y. Shotland, Glycerol as a green solvent for high product yields and selectivities, Environ. Chem. Lett. 5 (2) (2007) 67–71.
[16] Y. Gu, F. Jerome, Glycerol as a sustainable solvent for green chemistry, Green Chem. 12 (7) (2010) 1127–1138.
[17] C. Clavero, Plasmon-induced hot-electron generation at nanoparticle/metal-oxide interfaces for photovoltaic and photocatalytic devices, Nat. Photon. 8 (2) (2014) 95–103.
[18] W. Hou, S.B. Cronin, A review of surface plasmon resonance-enhanced photocatalysis, Adv. Funct. Mater. 23 (13) (2013) 1612–1619.
[19] E. Liu, L. Qi, J. Bian, Y. Chen, X. Hu, J. Fan, H. Liu, C. Zhu, Q. Wang, A facile strategy to fabricate plasmonic Cu modified TiO2 nano-flower films for photocatalytic reduction of CO2 to methanol, Mater. Res. Bull. 68 (2015) 203–209.
[20] E. Liu, Y. Hu, H. Li, C. Tang, X. Hu, J. Fan, Y. Chen, J. Bian, Photoconversion of CO2 to methanol over plasmonic Ag/TiO2 nano-wire films enhanced by overlapped visible-light-harvesting nanostructures, Ceram. Int. 41 (1, Part B) (2015) 1049–1057.
[21] W. Hou, W.H. Hung, P. Pavaskar, A. Goeppert, M. Aykol, S.B. Cronin, Photocatalytic conversion of CO2 to hydrocarbon fuels via plasmon-enhanced absorption and metallic interband transitions, ACS Catal. 1 (8) (2011) 929–936.
[22] Ş. Neaţu, J.A. Maciá-Agulló, P. Concepción, H. Garcia, Gold–copper nanoalloys supported on TiO2 as photocatalysts for CO2 reduction by water, J. Am. Chem. Soc. 136 (45) (2014) 15969–15976.
[23] Q. Kang, T. Wang, P. Li, L. Liu, K. Chang, M. Li, J. Ye, Photocatalytic reduction of carbon dioxide by hydrous hydrazine over Au–Cu alloy nanoparticles supported on SrTiO3/TiO2 coaxial nanotube arrays, Angew. Chem. Int. Ed. 54 (3) (2015) 841–845.
[24] D. Kumar, A. Lee, T. Lee, M. Lim, D.-K. Lim, Ultrafast and efficient transport of hot plasmonic electrons by graphene for Pt free, highly efficient visible-light responsive photocatalyst, Nano Lett. 16 (3) (2016) 1760–1767.
[25] A.D. McFarland, C.L. Haynes, C.A. Mirkin, R.P. Van Duyne, H.A. Godwin, Color my nanoworld, J. Nanoworld Chem. Educ. 81 (4) (2004) 544A.
[26] X. Qu, L.J. Kirschenbaum, E.T. Borish, Hydroxyterephthalate as a fluorescent probe for hydroxyl radicals: application to hair melanin, Photochem. Photobiol. 71 (3) (2000) 307–313.
[27] B. Zhou, J. Song, H. Zhou, L. Wu, T. Wu, Z. Liu, B. Han, Light-driven integration of the reduction of nitrobenzene to aniline and the transformation of glycerol into valuable chemicals in water, RSC Adv. 5 (46) (2015) 36347–36352.
[28] P.K. Jain, W. Qian, M.A. El-Sayed, Ultrafast electron relaxation dynamics in coupled metal nanoparticles in aggregates, J. Phys. Chem. B 110 (1) (2006) 136–142.
[29] A. Villa, N. Dimitratos, C.E. Chan-Thaw, C. Hammond, L. Prati, G.J. Hutchings, Glycerol oxidation using gold-containing catalysts, Acc. Chem. Res. 48 (5) (2015) 1403–1412.
[30] Y. Kim, D. Dumett Torres, P.K. Jain, Activation energies of plasmonic catalysts, Nano Lett. 16 (5) (2016) 3399–3407.
[31] M. Valenti, A. Venugopal, D. Tordera, M.P. Jonsson, G. Biskos, A. Schmidt-Ott, W.A. Smith, Hot carrier generation and extraction of plasmonic alloy nanoparticles, ACS Photon. 4 (5) (2017) 1146–1152.
[32] I.A. Shkrob, M.C. Sauer, Hole scavenging and photo-stimulated recombination of electron-hole pairs in aqueous TiO2 nanoparticles, J. Phys. Chem. B 108 (33) (2014) 12497–12511.
[33] V. Subramanian, E. Wolf, P.V. Kamat, Semiconductor-metal composite nanostructures. to what extent do metal nanoparticles improve the photocatalytic activity of TiO2 films? J. Phys. Chem. B 105 (46) (2001) 11439–11446.
[34] A.M. Nowicka, U. Hasse, M. Hermes, F. Scholz, Hydroxyl radicals attack metallic gold, Angew. Chem. Int. Ed. 49 (6) (2010) 1061–1063.
[35] G. Dodekatos, H. Tuysuz, Plasmonic Au/TiO2 nanostructures for glycerol oxidation, Catal. Sci. Technol. 6 (19) (2016) 7307–7315.
[36] J.A. Sullivan, S. Burnham, The selective oxidation of glycerol over model Au/TiO2 catalysts — the influence of glycerol purity on conversion and product selectivity, Catal. Commun. 56 (2014) 72–75.
[37] A. Mills, N. Wells, C. O'Rourke, Correlation between the photocatalysed oxidation of methylene blue in solution and the reduction of resazurin in a photocatalyst activity indicator ink (Rz Paii), J. Photochem. Photobiol. A 330 (2016) 86–89.
[38] M. Rochkind, S. Pasternak, Y. Paz, Using dyes for evaluating photocatalytic properties: a critical review, Molecules 20 (1) (2015) 88.
[39] Q. Xiang, J. Yu, P.K. Wong, Quantitative characterization of hydroxyl radicals produced by various photocatalysts, J. Colloid Interface Sci. 357 (1) (2011) 163–167.